Recent Res. Devel. in Plant Physiol., 1 (1997)

Approaches to understand signal-triggered responses of the plant cytoskeleton

Peter Nick, Qi-Yan Wang and Andreas Freudenreich
Institut für Biologie II, Schänzlestr. 1, 79104 Freiburg, Germany

To cope with environmental changes, plants have chosen a survival strategy that is based upon a remarkable developmental plasticity enabling them to tune their morphogenesis with signals perceived from the environment. On the cellular level, signals such as light, gravity, or hormones, can interfere with the control of cell shape. To fulfill this function, plants have evolved specialized cytoskeletal arrays (**Fig. 1**): cortical microtubules, preprophase band, and phragmoplast.

1. The role of microtubules in the control of cell shape

Microtubules seem to interfere with cell shape at the level of cell division, and at the level of cell expansion.

Spatial control of cell division. Cell division is heralded by a nuclear migration towards the site of the prospective cell plate (**Fig. 1**), and by the formation of an equatorial band of microtubules adjacent to the plasma membrane; the preprophase band (43). Although these microtubules disappear with the appearance of the division spindle, the preprophase band seems to predict symmetry and axis of the ensuing cell division: The spindle axis will be laid down perpendicular with the preprophase band (although it may subsequently be tilted due to space restrictions (46)) and the new cell plate will always form in the site predicted by the preprophase band. This is especially impressive with cell divisions that are asymmetric such as those observed during the formation of stomata or trichomes.

If the establishment of the preprophase band is disturbed either by mutations or by experimental manipulation, cell division can still proceed, though. However, axis and symmetry are dramatically disturbed.

This is illustrated by the *Arabidopsis* mutant *ton* (82), where the preprophase band is absent. The ordered pattern of cell division observed during the development of wild-type seedlings

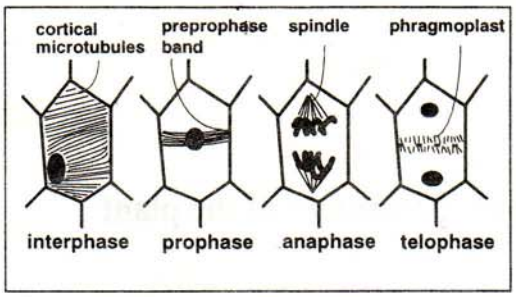

Figure 1: Microtubule arrays during the cell cycle of higher plants. Cortical microtubules, the preprophase band, and the phragmoplast are exclusively found in plants.

appears to be completely randomized in the mutant.

In apical cells of fern protonemata, the formation of the preprophase band can be manipulated either by cold treatment (causing depolymerization of microtubules) or by centrifugation of the nucleus towards the basal end of the cell (51). If these manipulations were performed during an early stage, a new preprophase band was established in the cell base and, subsequently, the new cell plate formed there. If the nucleus was centrifuged at a later stage (when a preprophase band had already been formed in the cell apex), a second preprophase band was found in the cell base and the new cell plate developed randomly with respect to orientation and symmetry. These experiments demonstrate that (i) the nucleus induces and guides the formation of the preprophase band, and (ii) that the correct formation of the preprophase band is a prerequisite for the spatial control of cell division.

Spatial control of cell elongation. A second plant-specific population of microtubules seems to be involved in the spatial control of cell expansion. The driving force for plant growth originates from the pressure exerted by vacuole and cytoplasm upon the cell wall. Pressure as such is not directional, and the cell is expected to grow isotropically. This is indeed observed in protoplasts, emphasizing the importance of the cell wall in the spatial control of cell expansion.

Anisotropic cell expansion, characteristic for cell-shape control, requires a kind of directional control of expansibility. A cylindrical cell is expected to expand preferentially in the lateral, not in the longitudinal axis (25). A „reinforcement mechanism" has been demonstrated in elongating cells that involves transverse deposition of cellulose microfibrils. In fact, elongating cells are characterized by transverse microfibrils, at least in the newly deposited inner wall layers, whereas a loss of this transverse orientation results in isodiametric or even lateral cell expansion (23, 25).

In most cases investigated so far, cortical microtubules have been found to be arranged in parallel to the newly deposited cellulose microfibrils (39). This is especially impressive in cells,

where the direction of microtubules changes in response to signals such as ethylen (37), auxin (5) or light (81). This parallelity between cortical microtubules and microfibrils culminated in the concept of the microtubule-microfibril hypothesis. This hypothesis assumes that cortical microtubules serve as guiding tracks for the cellulose-synthetizing enzyme complexes residing in the plasma membrane. Although this hypothesis is only an approximation to a far more complex reality (23, 70, 89), it is supported by a wealth of correlative data and can explain the frequent observation that the axis of cell expansion is lost after treatment with microtubule-eliminating drugs (3, 5, 64).

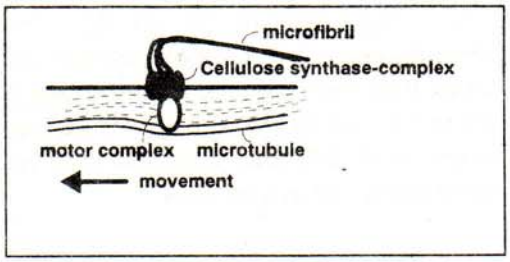

Figure 2: The microtubule-microfibril hypothesis in its simple version, where microtubules guide the movement (possibly driven by motor proteins) of cellulase synthase rosettes in the plasma membrane. Alternative models propose that the complexes are not physically linked to microtubules, but that microtubules produce membrane protrusions that direct the crystallization of cellulose.

The microtubule-microfibril hypothesis provides an attractive framework for approaches to signal-triggered cell-shape control in plants: Cortical microtubules can reorient swiftly in response to a range of signals such as blue light (38, 56), red light (81, 94), auxin (56), gravity (6, 56), and a range of plant hormones (74). This reorientation of cortical microtubules is then accompanied by a reorientation of cellulose deposition and a change of expansional axiality.

2. Microtubule reorientation and tropism.

Do microtubules control tropistic curvature? Supportive evidence The coleoptile is a specialized ephemeric organ in Graminean seedlings. It sheaths the primary leaves in germinating seedlings and protects them until they reach the soil surface. Upon illumination by day light, it terminates growth and the primary leaves subsequently pierces the coleoptile tip.

The coleoptile has been a favourite object of plant physiology since Darwin and Darwin (16) described the swift phototropic response of this organ. It can grow very fast, responds rapidly to environmental stimuli such as light or gravity and it enlarges exclusively by cell expansion. The photo- and gravitropic responses have been studied intensively during the first half of this century.

Two researchers (Cholodny and Went) demonstrated independently for gravitropism (12) and for phototropism (87)

that tropistic stimuli cause a shift of a growth-promoting factor across the coleoptile. The Cholodny-Went theory claims that the depletion of this factor in one flank causes an inhibition of growth, whereas growth is stimulated in the opposite flank of the coleoptile, where this factor becomes enriched. This work, eventually, lead to the isolation of the first plant hormone, auxin (88).

In coleoptiles that grow straight, the target for the action of auxin seems to be the epidermis. The expansion of the inner tissues is constrained by the relatively low extensibility of the outer epidermis, and auxin appears to act by releasing this constraint (35).

In coleoptiles that undergo rapid elongation, cortical microtubules are found to be transverse in both, the cells of the inner tissue and in the epidermis (maize: 56, rice: 81). Consistently, cellulose microfibrils are deposited in transverse direction reinforcing the elongation of the cell (maize: 5, rice: 81).

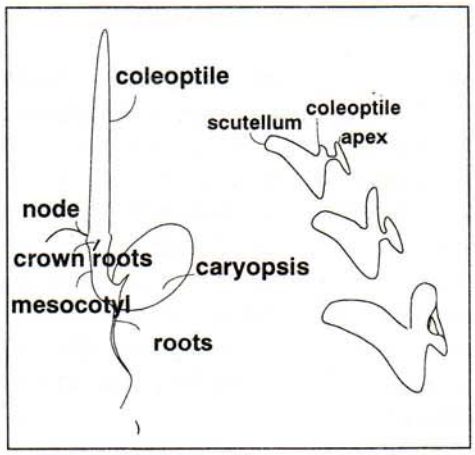

Figure 3: The Graminean coleoptile (left) develops during late embryogenesis from the base of the scutellum (right).

If the coleoptile tip (the major source of auxin) is excised and the cells are depleted from endogenous auxin by incubation of coleoptile segments in water, microtubules change their orientation from transverse to longitudinal and the cellulose-microfibrils are deposited in longitudinal direction (5). This results in a loss of growth reinforcement and, consequently, in a block of coleoptile elongation. This process is reversible by addition of exogenous indole-acetic acid (5, 56, 61, 63). The time course of this phenomenon reveals that microtubules respond within 10 to 15 min to the addition of indole-acetic acid (56) and complete their reorientation within one hour.

Phototropic (or gravitropic) stimulation of intact coleoptiles induces a reorientation of cortical microtubules in the lighted (or upper) flank, whereas the microtubules in the shaded (or lower) flank reinforce their transverse orientation (56). This gradient of microtubule orientation is correlated with a gradient of growth (inhibition of growth in the flank, where microtubules are longitudinal, stimulation of growth in the flank, where microtubules are transverse) resulting in tropistic bending (**Fig. 4**).

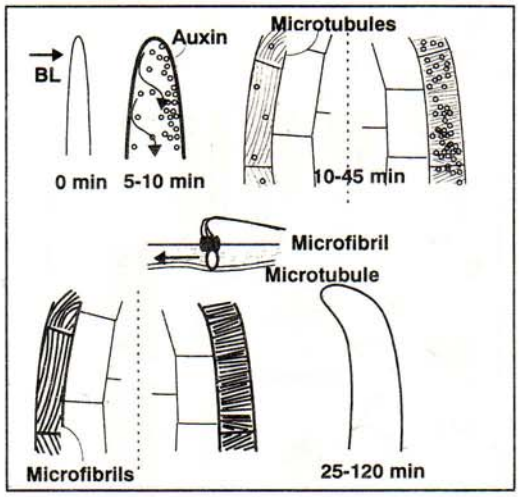

Figure 4: Original model on the role of microtubules in phototropism (according to 56). Phototropic stimulation causes a displacement of auxin towards the shaded side of the coleoptile. Auxin depletion in the lighted side results in reorientation of microtubules from transverse to longitudinal and longitudinal deposition of cellulose microfibrils. This leads to a decrease of epidermal extensibility and reduced growth. The growth gradient eventually results in tropistic bending towards the light.

These observations can be interpreted in the following ways (**Fig. 5**):

(i) Tropistic stimulation causes a displacement of auxin across the coleoptile (Cholodny-Went theory). The auxin gradient results in a gradient of microtubule orientation yielding asymmetric growth (**Fig. 5A**).

(ii) The auxin gradient causes asymmetric growth that causes the reorientation of microtubules in the side that is growing slower (**Fig. 5B**).

(iii) The auxin gradient causes asymmetric growth and a gradient of microtubule orientation in two parallel, but independent steps (**Fig. 5C**).

The time course of the phototropically induced microtubule reorientation speaks against the second possibility: microtubule reorientation becomes detectable from 10 min after stimulation and is complete within one hour -

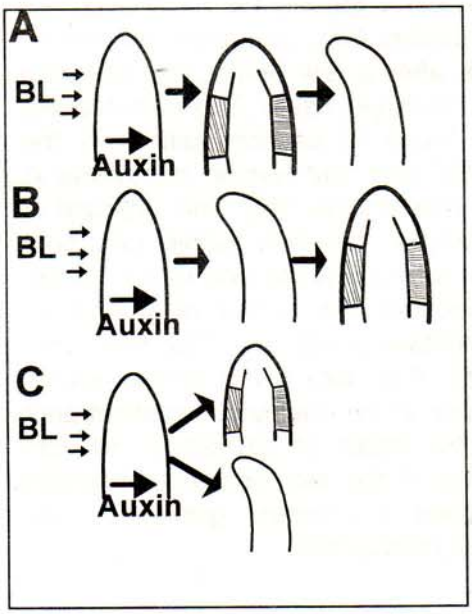

Figure 5: Possible alternatives for the relation between asymmetric growth and the gradient of microtubule orientation induced by phototropic stimulation. The orientation gradient causes the growth gradient **(A)**, the growth gradient causes the orientation gradient **(B)**, both gradients develop in parallel, but independently of each other **(C)**.

phototropic curvature becomes detectable from 20 to 30 min after stimulation and reaches a maximum at two hours after stimulation (56).

Do microtubules control tropistic curvature? Contradicting evidence
The following observations favour the third possibility over the first (60):

(i) Following phototropic stimulation by a pulse of blue light curvature reaches a maximum at two hours after stimulation. Caused by gravitropic counterstimulation experienced by the curved coleoptiles (53), coleoptiles straighten, and, after a few hours, the curvature has vanished again. The microtubules are found to be longitudinal in the lighted side, but remain transverse in the shaded side (60). This gradient of orientation develops within one hour after the light pulse and is maintained throughout the period of gravitropic straightening (**Fig. 6A**). The first hypothesis (**Fig. 5A**) would predict an inversion of the orientation gradient prior to the onset of gravitropic straightening, if the two tropistic responses produce asymmetric growth by the same mechanism.

(ii) If maize coleoptiles are rotated on a horizontal clinostat in the absence of tropistic stimulation, a nastic curvature develops in the dorsiventral axis of the coleoptile (54). This curvature is strong, when the coleoptiles are symmetrically irradiated by red light, it becomes weaker, when the plants are

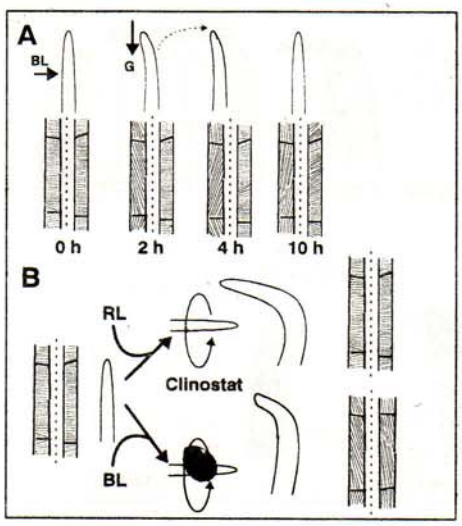

Fig. 6: The behaviour of microtubules during gravitropic straightening **(A)** and during nastic curvature **(B)** does not support the model shown in **Fig. 4**.

irradiated by blue light. Under red light, the microtubules are transverse on both flanks of the bending organ, they are longitudinal under blue light (**Fig. 6B**). In none of the two cases any gradient of microtubule orientation across the organ could be detected (60). The first hypothesis (**Fig. 5A**) would predict that microtubules are found to be more longitudinal in the slower growing side.

(iii) When, two hours after a phototropic stimulus, the coleoptiles are subjected to a phototropic counterstimulation of equal strength, but opposing direction, and the coleoptiles are rotated on a clinostat (to exclude gravitropic coun-

terstimulation), they interrupt their bending towards the first stimulus and start bending towards the counterstimulus (53). This dominance of the counterstimulus is transient, though: Already one hour later, the coleoptiles „remember" the direction of the first stimulus and return to their original mode of curving, that is subsequently maintained for many hours (60, 63). The orientation of microtubules is longitudinal in the side that had been hit by the first stimulus. In contrast to bending itself, microtubules do not respond at all to the second, opposing light (60, 63). The first hypothesis (**Fig. 5A**) would have predicted an inversion of the orientation gradient in response to the counterstimulus and a second inversion back to the original gradient.

These observations indicate that a gradient of microtubule orientation is neither necessary (**Fig. 6B**) nor sufficient (**Fig. 6A,B**) for asymmetric growth. In other words: microtubule orientation and curvature appear not to be causally linked but to develop as parallel phenomena (**Fig. 5C**).

Microtubules are the expression of a stable transverse polarity. The bending response to blue light is transient, reaching a maximum at two hours after induction and disappearing subsequently (53). However, if gravitropic stimulation is made symmetrical by rotation on a horizontal clinostat, a stable bending towards the inducing pulse is observed. If the coleoptiles are transferred to the clinostat only after the phototropic bending had disappeared due to gravitropic straightening, nevertheless a stable curvature in direction of the first pulse develops **(Fig. 7)**. This demonstrates the existence of a spatial memory that had been induced by the stimulus and that persisted even during the time of gravitropic straightening. This spatial memory can thus be separated from bending itself.

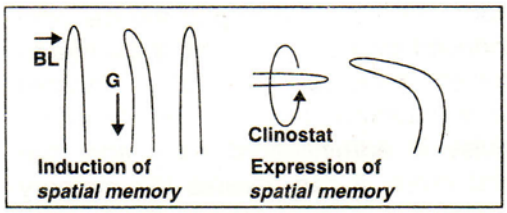

Figure 7: Demonstration of a stable spatial memory that is induced by phototropic stimulation (according to 53).

Similar directional memories have been repeatedly described for both gravitropism (7, 15) and phototropism (26). In order to detect a directional memory following tropistic stimulation, the expression of the tropistic response was suppressed by cold (15), by auxin depletion (7) or by specific ion-channel blockers (26). If the suppressive treatment was eventually removed, the response to the stimulus developed.

Such experiments indicate that the stimulus can induce a transverse polarity that can be separated from its expression as curvature and can per-

sist over a long time even if it is prevented from becoming manifest. The suppressive condition in case of the phototropic memory of maize coleoptiles is the gravitropic counterstimulation experienced by curved coleoptiles - it is removed by clinostat rotation allowing for expression of the memory as stable bending (53).

When does the spatial memory become stable? This question can be addressed by challenging the memory induced by a stimulus with a counterdirected stimulus given after variable time intervals (53). If the opposing pulse is administered early after the first pulse, it can reverse the memory completely and a strong stable bending response towards the second pulse is observed (**Fig. 8A**, upper lane). If the opposing pulse is administered later, it fails to reverse the memory. It first does reverse, however, the bending response (**Fig. 8A**, lower lane). This reversal of the sign of bending remains transient though, and subsequently the original response (directed towards the first pulse) is restored and maintained over a long time (53). A similar spatial memory can be induced by gravitropic stimulation (**Fig. 8B**).

A detailed fluence-response study for the first and the second stimulation (58) demonstrated that, independently of fluence, the spatial memory becomes irreversibly fixed at two hours after the first, inducing pulse. This fixation time is independent of the interaction between the two stimuli and the direction of the spatial memory.

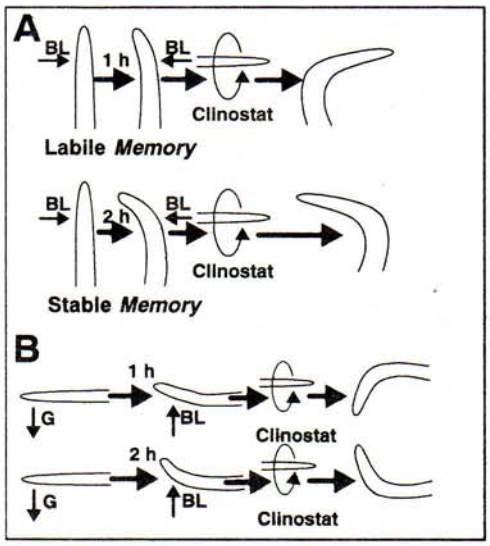

Fig. 8: Experiment to determine the stability of the spatial memory induced by phototropic **(A)** or gravitropic **(B)** stimulation according to 53 and 60).

The gradient of microtubule orientation seems to be tightly correlated to the establishment and fixation of this spatial memory:

(i) The orientation gradient (60) as well as the spatial memory (53)) persist during gravitropic straightening.
(ii) The orientation gradient (60, 63) as well as the spatial memory (53, 63) do not respond - in contrast to curvature - to a phototropic counterstimulus that is administered late (two hours) after the inducing pulse.
(iii) The orientation gradient (63) as

well as the spatial memory (53, 58) can be reversed by a counterstimulus that is administered early (one hour) after the first pulse.
(iv) The orientation of microtubules is irreversibly fixed at the same time, when the spatial memory is irreversibly fixed (58, 63).

These observations suggest that the reorientation of microtubules is the cellular expression of spatial memory, and that the fixation of microtubule orientation is the cellular correlate to the irreversible fixation of this memory.

A further characterization indicated that the blue-light effect on microtubule reorientation is mediated by auxin (63), whereas the blue-light induced fixation of microtubule orientation is not mediated neither by auxin nor by a gradient of auxin. The blue-light induced fixation of microtubules does not require a light gradient and resides in the coleoptile base as shown by partial irradiation using a light pipe. The perception for the blue-light induced reorientation of microtubules, in contrast, resides in the coleoptile tip.

The results of this analysis can be summarized as follows: Tropistic stimulation triggers three chains of events (**Fig. 9**):
(i) Perception in the coleoptile tip causing a displacement of auxin towards the shaded side, resulting in inhibition of cell elongation in the lighted side and stimulation of growth in the shaded side (30). The asymmetric growth causes then the bending towards the light.
(ii) Reorientation of microtubules, caused by a displacement of auxin.
(iii) Perception in the coleoptile base triggering the production of a factor (that is independent of auxin) that can fix microtubules (irrespective of their actual orientation). This fixed microtubule orientation seems to be the cellular base of a stable transverse polarity that can be rendered manifest by clinostat rotation.

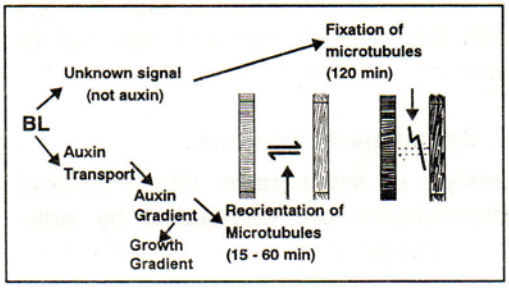

Figure 9: Signal chains that are triggered by phototropic stimulation. Blue light induces lateral auxin transport resulting in a gradient of auxin causing a gradient of growth and, in parallel, a gradient of microtubule orientation. A second signal that is not carried by auxin causes fixation of microtubule orientation two hours after irradiation.

To attain access to the molecular base of stimulus-triggered microtubule responses, two approaches were developed in parallel:

(i) A search for mutants, where the cytoskeletal response to triggering stimuli is altered.

(ii) A search for proteins that interact with the cytoskeleton and respond to environmental signals.

2. Cytoskeletal mutants

Design of the screen. When cortical microtubules are eliminated by anti-microtubular drugs such as colchicine (5), oryzalin (3), propyzamide or ethyl-N-phenylcarbamate (73), this results in a loss of cell axiality and, consequently, in a block of elongation. In addition, the gravitropic response becomes impaired (59). These drugs exert their effect by binding to tubulin dimers and preventing them from being added to the growing end of polymerizing microtubules - they do not really disrupt microtubules (48).

The effect of these microtubule-eliminating drugs depends on the natural turnover of microtubules: after inhibition of polymerization microtubules will shrink due to the dynamics of assembly and disassembly. The more dynamic a microtubule, the more sensitive it will be to the drug. Conversely, resistance to the drugs can be caused by a decreased turnover of microtubules. Resistance of cell elongation to anti-microtubular drugs provides a selectable marker for reduced microtubule turnover (64). In addition, this screen should recover mutations for drug uptake and drug-binding of mutated tubulin isotypes.

Such a screen was initiated in rice: rice has the smallest genome of all Gramineae (2), the physiology of rice has been studied for almost a century, it is readily accessible to biochemical and molecular analysis, and the entire rice genome will soon be mapped (34) and even sequenced in frame of the Japanese Rice Genome Project. Moreover, rice is the most important crop with a tremendous cultural and economic impact especially in Asian countries.

The screen was designed as a lethal-mutant screen (**Fig. 10**), i.e. individual plants were treated as separate lines during screening of the F_2 generation of plants that had been mutagenized by γ-rays.

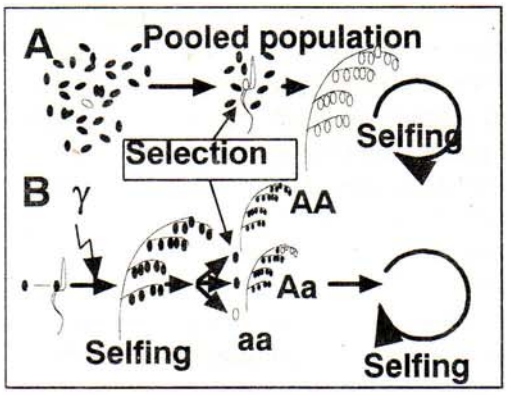

Figure 10: Conventional screen of pooled populations **(A)**, and lethal-mutant screen **(B)**. In a lethal-mutant screen individual plants are treated as separate lines. If the homozygous mutants (aa) are sterile, the line can be maintained by the heterozygotes (Aa).

Aliquots of more than 7000 individual lines were tested for resistance of coleoptile elongation and gravitropism

to the microtubule polymerization blocker ethyl-N-phenylcarbamate (47, 48). The drug treatment blocked elongation of coleoptiles and roots in seedlings of the wild type and caused distorted growth due to a block of coleoptile gravitropism (64, 67). Resistant mutants were characterized by elongating coleoptiles that grew vertically (64). They were raised to maturity and their offspring was tested for inheritance of the trait. The selection was repeated for the third generation as well, leaving 35 resistant lines.

As expected, some of these mutations (presumably affecting the cytoskeleton) had dramatic effects on development leading, in the extreme, to lethality or sterility. In those cases, the lethal-mutant approach allowed to maintain the line by propagation of the heterozygotes (**Fig. 10**).

Among those lethal or sterile mutants were *Störtebeker* (lacking the aerial parts of the seedling), *futago* (with a duplication of the entire seedling axis, **Fig. 11A**), *Doppelkopf* (duplication of coleoptile and primary leaves), *hebiba* (lacking the phytochrome-mediated inhibition of coleoptile elongation, exhibiting hypertrophic elongation of leaves and degeneration of female organs, **Fig. 11B**), and *ER31* (exhibiting short coleoptiles and long mesocotyls, **Fig. 11C**).

***ER31* is affected in auxin-dependent microtubule-reorientation.** The mutant *EPC-resistant 31* (*ER31*) was one

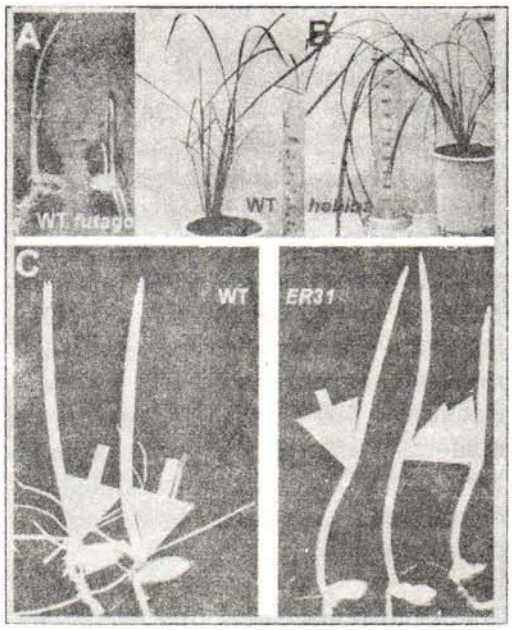

Fig. 11: Panel of isolated rice mutants. **(A)** *futago* with doubled seedling axis, **(B)** *hebiba* mutant exhibiting hypertrophic leaf elongation, and **(C)** *ER31* with reduced coleoptile and enhanced mesocotyl elongation.

of the mutants that were lethal in the homozygous state. In heterozygotes, however, it was found to confer increased resistance of coleoptile and mesocotyl elongation to EPC (64). In absence of the drug, the heterozygotes developed coleoptiles that were shorter than in the wild type by about a third), whereas the mesocotyl was dramatically prolonged (**Fig. 11C**. These changes in elongation could be attributed to a changed pattern of cell elongation: The cells in the coleoptile are much shorter, the cells in the mesocotyl much longer as compared to

the cells of the wild type (64).

The orientation of cortical microtubules was altered as well (64): In the coleoptile, microtubules in epidermal cells were found to be longitudinal (as compared to almost transverse microtubules in the wild type), and slightly oblique in the subepidermis (as compared to strictly transverse microtubules in the wild type. In the mesocotyl, microtubules were found to be more transverse than in the wild type, in the epidermis as well as in the subepidermis. The pattern of microtubule orientation is thus parallel to the pattern of cell elongation.

In coleoptile segments, the microtubules withstood treatment with EPC as well as a treatment with the microtubule-depolymerisation blocker taxol (68). This indicates that the mutation caused a reduced turnover of microtubules (64).

It was not possible to induce transverse microtubules by treatment with auxin in the epidermis of *ER31* coleoptiles, whereas the microtubules in the wild type responded readily to auxin (64). This might be caused by an impaired ability of the mutant to sense or to process the auxin signal. However, the dose-response curve for auxin-induced callus formation (64) as well as the dose-response curve for short-term growth (up to three hours) of coleoptile segments (**Fig. 12**) did not reveal any defect in the sensitivity or the responsiveness of *ER31* to auxin.

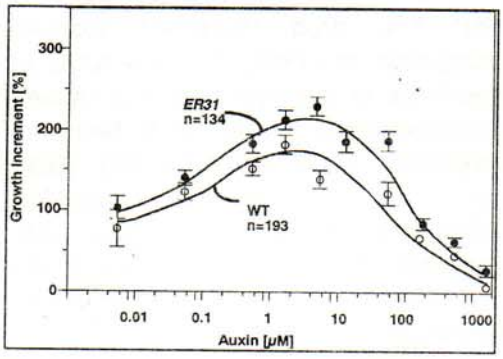

Figure 12: Dose-response relation for auxin-dependent elongation of coleoptile segments in wild-type and *ER31*.

Alternatively, the microtubules could be impaired in their ability to assume a transverse orientation or in their ability to reorient at all. Interestingly, it is possible to cause a reorientation by other signals (64): in subepidermal cells by gibberellin (inducing reorientation from oblique to transverse) or by red light (inducing reorientation from oblique to longitudinal), in the epidermis by gravitropic stimuli (inducing reorientation from longitudinal to transverse at the lower flank). This suggests that the components necessary for microtubule reorientation are present. Moreover, microtubules in the mesocotyl are transverse (in contrast to the almost longitudinal microtubules of the wild type).

These data suggest that *ER31* is impaired in the coupling between the auxin-triggered signal chain and the

reorientation of microtubules (**Fig. 13**). A working hypothesis assumes that auxin controls the balance between disassembly and assembly of microtubules that seems to be a prerequisite for reorientation (93). The lack of a microtubular response to EPC and taxol in *ER31* coleoptiles indicates a reduced rate of microtubule turnover in response to auxin. By microinjection of fluorescent tubulin into living pea epidermis it has been demonstrated (93) that orientation-dependent differences in the balance between assembly and disassembly play a pivotal role in the reorientation of cortical microtubules.

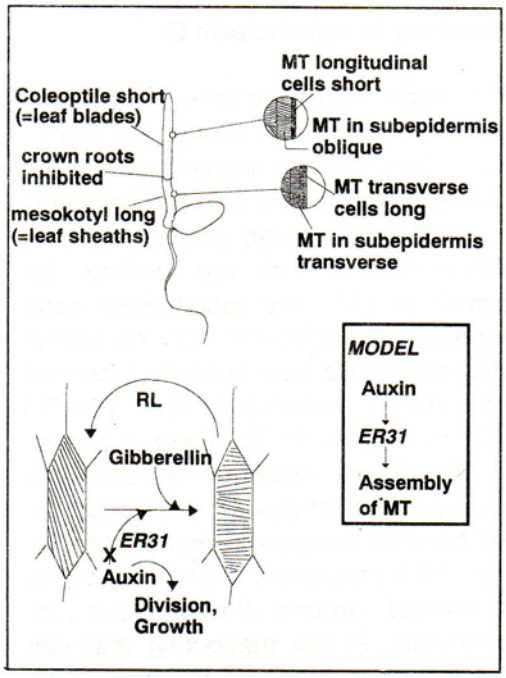

Figure 13: Summary of the *ER31* phenotype and working hypothesis on the target of the mutation. Model according to 64.

Future work will be dedicated to the identification of the mutated gene and the investigation of the pattern of microtubule-associated proteins (MAPs) in ER31. In addition, the mutant can be used to evaluate the role of microtubule reorientation for various growth and developmental responses.

***Yin-Yang* is affected in auxin-dependent actin dynamics.** The *Yin-Yang* mutant was selected as a second-site mutation in the EPC-resistant line *störtebeker*. Pure lines of *Yin-Yang* show a peculiar coloration of the endosperm that is divided into an opaque upper and a translucent lower half. This coloration and the other traits of the *Yin-Yang* phenotype (see below) are inherited in a Mendelian way with complete dominance of the wild-type over the mutant allele.

Seedlings of the mutant are characterized by a stimulation of mesocotyl length to more than two-fold and a slight promotion (by about one third) of coleoptile elongation. The changes in mesocotyl growth can be completely attributed to a stimulation of cell elongation, probably related to a more transverse arrangement of microtubules (86).

Surprisingly, the cells of the coleoptile epidermis are not longer, but clearly shorter than in the wild type. The enhanced coleoptile length is caused by an increased number of cells rather than an increase in the elongation of

cells. It was expected that this should be accompanied, in a way similar to *ER31*, by a microtubule orientation that is more longitudinal as compared to the wild type. This is not the case: Microtubules are more transverse in the epidermis of *Yin-Yang* coleoptiles and therefore should allow for a more pronounced elongation than in the wild type.

In aerially grown coleoptiles of rice, elongation is controlled by auxin (22) as in other Graminean species. The impeded elongation of the *Yin-Yang* coleoptile might be caused by a reduced sensitivity of the tissue to auxin. However, the dose-response curve for auxin-dependent elongation of coleoptile segments does not reveal any differences in threshold or optimal concentrations between *Yin-Yang* and the wild type (86). Interestingly, the amplitude of the response appears to be enhanced in *Yin-Yang*, indicating that in the mutant the capacity for elongation is increased when the limitation by auxin is released.

A pharmacological analysis of the mutant responses revealed that auxin-induced elongation in *Yin-Yang* exhibits an increased sensitivity of coleoptile growth to the actin-polymerization blocker cytochalasin D (**Fig. 14**). Surprisingly, this increased sensitivity requires the presence of auxin to become manifest. Below a threshold of 200 nM of indole-acetic acid, the mutant does not exhibit this increased sensitivity to cytochalasin D.

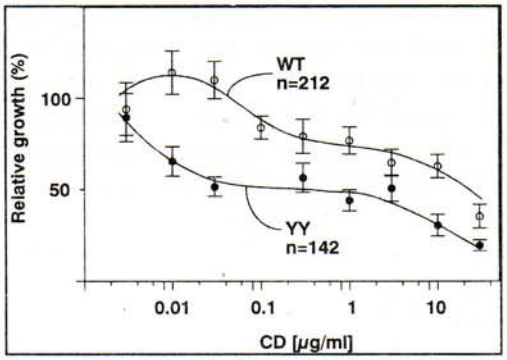

Figure 14: Differential sensitivity of auxin-induced elongation to the actin-polymerization blocker cytochalasin D in wild type and *Yin-Yang*. Coleoptile segments were incubated for 3 hours in presence of 5 µM indole-acetic acid.

The actin microfilaments in the epidermis of intact coleoptiles are significantly less bundled as compared to the wild type (86). Upon addition of auxins such as indole-acetic acid or 2,4 D in concentrations that are optimal for growth (5 µM), the longitudinal actin bundles characteristic for epidermal cells of the wild type become loosened and reveal numerous fine parallel strands of actin. In *Yin-Yang*, a dramatically altered response is observed upon addition of auxins: The longitudinal bundles disappear almost completely and a meshwork of short filaments is formed around the nucleus. Interestingly, in the mesocotyl that can be induced to elongate by gibberellins (62), gibberellin can trigger a similar response in Yin-Yang, but not in the wild type (86).

A similar „nuclear basket" can be induced in the wild type by blockers of actin polymerization such as cytochalasin D or cytochalasin B, consistent with published results from other cell types (78). Thus, in *Yin-Yang*, auxin causes effects that are found in the wild type following a treatment with cytochalasin D. It should be mentioned that, in *Yin-Yang*, the gravitropic bending initiates earlier and that a similar shift of the response lag is observed in the wild type after pretreatment with cytochalasin D (67).

These aspects of the *Yin-Yang* phenotype (**Fig. 15**) indicate that a

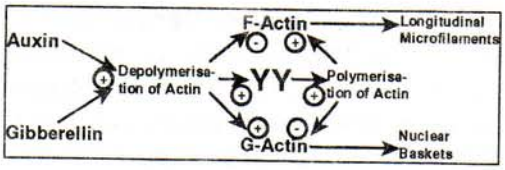

Figure 15: Possible function for the gene product (YY) of the *Yin-Yang* gene. Growth stimulating signals such as auxin or gibberellin cause in increased depolymerization of actin that is balanced by an increased polymerization (mediated by the YY gene product). In the mutant, the pool of G-actin increases in response to auxin and is assembled into short filaments around the nucleus.

factor that is required for actin polymerization becomes limiting in *Yin-Yang* under conditions of stimulated actin turnover (as induced by auxin, see 80).

Outlook: Interaction of actin and microtubules in the control of cell growth. The mutant analysis supports the notion that microtubule reorientation is not sufficient to explain growth responses to environmental stimuli:

(i) Despite the lacking response of microtubules to auxin in *ER31*, auxin can induce elongation in coleoptile segments of this mutant (**Fig. 12**).
(ii) Despite a transverse orientation of microtubules in *Yin-Yang* that should support enhanced cell elongation, cell growth is impeded in this mutant. The phenotype of the *Yin-Yang* mutant points to the possibility that actin microfilaments could play a pivotal role in the control of cell elongation.

At the time, the role of actin microfilaments could be accomodated into the following working hypotheses:

(i) The thick longitudinal actin bundles characteristic for epidermal cells physically link the cell poles. Auxin can loosen this links and allows the cell poles to be move apart. Direct measurements of the mechanical properties of microfilaments in cell cultures using optical tweezers demonstrate that, in fact, microfilament bundles become more extensible upon treatment with auxin (24).
(ii) The fine microfilaments observed in auxin-treated cells could serve as tracks for vesicle transport to the cell poles that would promote wall expansion or wall loosening there. Blockers of vesicle trafficking, such as Brefeldin A, have been shown to suppress root elongation (3).

(iii) Actin microfilaments might control and/or maintain the preferential orientation of cortical microtubules and thus interfere with cell shape. In several systems, microtubule orientation has been shown to change upon disruption of actin microfilaments (21, 55, 71).

The interaction between actin microfilaments and microtubules is far from being understood, but it is clear that molecules connecting these two components of the cytoskeleton might be the key targets for signal-triggered control of the cell shape.

4. Signal-regulated microtubule-associated proteins

The dynamic-helix model: reorientation by sliding? How do cortical microtubules reorient? With the development of immunofluorescence microscopy this question could be addressed for the first time. In contrast to the old work based on electron microscopy, it was now possible to visualize the cytoskeleton as an entity. This new technique revealed a remarkable spatial continuity of the cytoskeleton all over the cell producing, in many cells, helicoidal arrays of cortical microtubules (42). This observation led to a first, elegant, model of microtubule reorientation (42): By mutual sliding of microtubules this helix could contract, resulting in a steeper pitch, and oblique or even longitudinal arrays of microtubules (**Fig. 16**). Conversely, the helix could relax by sliding in the opposite sense, causing a more transverse orientation of microtubules. In neurons, indeed, a transport of entire microtubules along other microtubules has been demonstrated recently, supporting the dynamic-helix model (1).

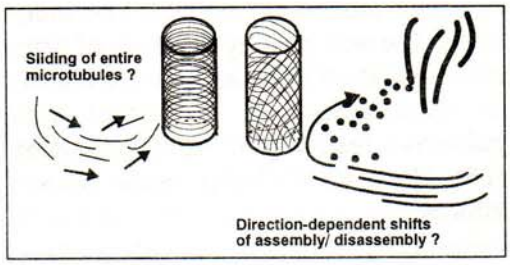

Figure 16: Alternative models to explain microtubule reorientation. The dynamic-helix model (42) assumes that microtubules are mutually sliding, thus changing the pitch of the helicoidal array. The directional assembly model (90, 93) assumes that the dynamic equilibrium between assembly and disassembly becomes shifted in an orientation-dependent manner.

In the last years, however, evidence accumulated that at least confines the importance of mutual sliding for the reorientation of microtubules:

(i) in epidermal tissues, the orientation between the two flanks or a cell can differ, often resulting in a situation, where microtubules are longitudinal at the outer cell side, whereas they are transverse at the inner side (56, 66). Even in those cases, where the cytoskeleton seems to maintain continuity (90), it remains difficult to imagine, how, under these conditions, simple

sliding should result in a change of pitch. Moreover, electron microscopy suggests that the cross-distance between individual microtubules is considerable, which is difficult to reconcile with the sliding-helix model (89).

(ii) In several cases, the reorientation of microtubules can be impaired by taxol (19), a drug that binds to polymerized microtubules and inhibits microtubular breakdown (68). This suggests that microtubule depolymerisation is a necessary event during microtubule reorientation.

(iii) Cortical microtubules are more dynamic than hitherto assumed: By microinjection of fluorescent neurotubulin into living plant cells, it was possible to bleach patches of the now fluorescent cytoskeleton by a laser beam. The recovery of fluorescence in those patches could now be monitored as an indicator for the exchange of tubulin dimers (93). Surprisingly, this recovery was very fast, and the estimation for the rates of subunit exchange demonstrated that cortical microtubules are as dynamic as other microtubular arrays.

These observations allow for an alternative explanation of microtubule reorientation: Direction-dependent shifts in the balance between assembly and disassembly of microtubules instead of microtubule sliding (**Fig. 16**). If polymerization of, for instance, longitudinal microtubules were favoured over that of transverse microtubules, transverse microtubules are expected to disappear rapidly, due to their turnover, whereas longitudinal microtubules should become more abundant. It cannot be excluded that, in addition, sliding of microtubules contributes to reorientation. Nevertheless, the impact of direction-dependent shifts of assembly/disassembly as major driving force for microtubule reorientation is illustrated by several observations:

(i) Taxol blocks reorientation in cultured cells that possess a wall (19). This can be interpreted in terms of an drug-induced shift of the equilibrium towards maintenance of the *status quo*.

(ii) The EPC-resistant mutant *ER31* exhibits insensitivity to both EPC and taxol (64) indicating a reduced turnover of tubulin dimers. Interestingly, the microtubules of this mutant cannot reorient in response to auxin.

(iii) The transition state between transverse and longitudinal microtubules is not characterized by homogeneously oblique microtubules as predicted by the dynamic-helix model, but by a patchwork of intermingled areas with transverse and longitudinal microtubules (61).

(iv) If the reorientation from the transverse into the longitudinal array is monitored in living epidermal cells by microinjection of fluorescent neurotu-

bulin (93), a sudden disappearance of transverse microtubules is observed along with almost simultaneous formation of longitudinal microtubules.

Based on these considerations, it is necessary to ask two questions to understand microtubule reorientation on the molecular level:

(i) What factors control the equilibrium between microtubule assembly and disassembly?
(ii) Why and how does the abundance, activity or localisation of these unknown factors depend on direction?

The second question is more startling from a logical point of view and is far from being elucidated. However, there exist some observations and concepts dealing with the first question that might help to design a molecular approach for the second problem as well.

The formation of microtubules can be divided into two aspects: (A) establishment of new sites for microtubule nucleation, and (B) control of microtubule elongation.

Control of microtubule nucleation. In cells of animals and lower plants, the nucleation of microtubules is under control of specialized organelles, the centrosomes (10). Higher plants, with exception of the archaic tree *Gingko biloba*, do not possess centrosomes. In higher plants, the nucleation of microtubules is not concentrated in a specialized organelle, but occurs at multiple sites that are operationally defined as microtubule-organizing centers (MTOC). These MTOCs are thought to be subject to spatial and temporal control (36). Such a MTOC activity was shown, in cycling cells, in the nuclear envelope (79, 83, 95,). In differentiated cells, however, microtubule nucleation by sites that were adjacent to the plasma membrane have been reported that might be relevant for the nucleation of cortical microtubules (13, 20, 27, 45). The molecular composition of these MTOC is still unknown - it is worth mentioning, however, that γ-tubulin, a key component of the centrosome, has been detected in potential sites of microtubule nucleation in plants (41).

Control of microtubule elongation. In order to ensure directed outgrowth of microtubules from these nucleating MTOC, further factors must be present that stabilize microtubules and cross-link them to bundles, to other cytoskeletal components (such as actin microfilaments) or to membranes. In addition, the balance between assembly and disassembly of microtubules might be shifted by various tubulin isotypes (76) or by posttranslational modifications of tubulin (17):

In all plant species investigated so far, there exist several genes for both, α- and β-tubulins, and this corresponds to a manifold of tubulin isotypes on the protein level that exhibit subtle diffe-

rences in charge and possibly function (14). Although cortical microtubules seem to consist of mixed isotype populations (29), the developmental and tissue-specific expression of some isotypes (32) suggests that they might be related to the dynamic properties of microtubules. Moreover, several mutations of certain isotypes seem to confer resistance to antimicrotubular drugs (40).

The tubulin molecule itself is subject to numerous posttranslational modification such as acetylation, deglutamylation, or tyrosination, and some of these modifications have been correlated, in animal cells, with altered stability of microtubules. In plants, reduced tyrosination has been detected in the context of microtubule reorientation induced by the plant hormone gibberellin in pea (17). It is difficult, however, to assess, whether these changes are cause or consequence of altered microtubule stability, and it is not known, whether they are dependent on the orientation of microtubules.

Plant MAPs. In addition to these factors that are intrinsic to microtubules, the dynamics of assembly and disassembly can be controlled by extrinsic factors such as the activity of specific microtubule-associated proteins (MAPs). These proteins were first isolated from neural tissue by their ability to cofractionate with microtubules during repeated cycles of warm-induced assembly and cold-induced disassembly. They are able to stimulate formation of microtubules from purified tubulin *in vitro* (33). However, the decisive criterion for a microtubule-associated protein is the attachment of the protein to microtubules *in vivo* (77).

In plants, several proteins have been described as MAPs, although the term MAP has been under debate recently in this context (50). A 50-kDa microtubule-binding protein purified from carrot cell cultures has been identified as translation factor EF1-α (18) and seems to cause bundling of microtubules. In animal cells, however, EF1-α has been shown to be an actin-binding protein (91) that is involved in the binding of untranslated mRNA to the cytoskeleton (4). It is actin on microtubules as well, although not as a bundling protein but as a protein that causes fragmentation of microtubules (75). As a second potential plant MAP, the p86-subunit of the eucaryotic initiation factor-(iso)4F has been reported to mediate end-to-end annealing of microtubules (28).

In addition, a number of yet unidentified microtubule-binding proteins has been isolated from plant cells: A 100-kDa protein from tobacco BY-2 phragmoplasts can bind to microtubules in an ATP-dependent manner (92), and a 66-kDa protein from the same cell culture has been shown to associate with microtubules *in situ* (11). A heat-stable protein from green algae has been found to cause bundling of

microtubules (44), and a 50-kDa protein from mung beans links microtubules to potential elements of the intermediate filaments (49). A 34-kDa protein from mung bean is recognized by anti-idiotypic antibody raised against a conserved domain of neurotubulin and might be a MAP as well (31). Except for the two factors of the translation machinery, EF1-α (18) and IF-(iso)4F (28), those microtubule-binding proteins could not be identified - it is very difficult to purify sufficient amounts for microsequencing by approaches that are based on microtubule-binding or microtubule-coassembly.

A different approach was based on the property of many animal MAPs to be heat-stable. A heat-stable 100-kDa protein from maize Black Mexican Sweet cells was shown to bind to neurotubules and was recognized by an antibody raised against the animal MAP τ (85). By fractionating for heat stability, this protein, P_{100}, could be enriched and a polyclonal antibody could be raised against this protein.

Approaches to isolate plant MAPs. In neural tissues, MAPs have been identified by their capacity to cofractionate with microtubules during repeated cycles of cold-induced disassembly and warm-induced reassembly (72). In plant cells, the concentrations of tubulin reached in the extract is far below the critical concentration necessary for the assembly of microtubules. For this reason only one case been published so far (11), where a potential MAP could be detected by cofractionation with warm-induced microtubules. This required devacuolation of the cells prior to extraction in order to increase the proportion of cytoplasm in the extract. To overcome this drawback, essentially four approaches have been designed to purify plant MAPs (**Fig. 17**):

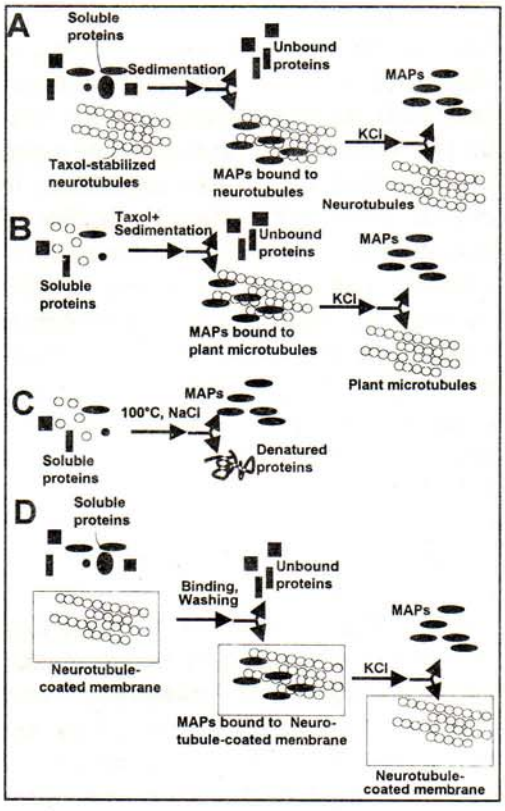

Figure 17: Methods to purify plant MAPs. Cosedimentation with taxol-stabilized neurotubules **(A)**, coassembly with endogenous plant tubulin **(B)**, thermostable extraction **(C)**, and neurotubule-affinity assay **(D)**.

(i) Taxol-stabilized neurotubules **(Fig. 17A)** are added to the extract as a „bait" to fish for binding proteins (85). Both, microtubules, and potential MAPs are then collected by centrifugation and subsequently the MAPs are detached from the sedimented neurotubules by salt.

(ii) To induce formation of microtubules at low concentrations of tubulin, taxol (**Fig. 17B**) is added to the soluble extract (65, 84). Taxol inhibits microtubule depolymerisation (68) and lowers the critical concentration of tubulin necessary for the formation of new microtubules. The microtubules, and the potential MAPs that have coassembled with them, can now be sedimented by centrifugation. The MAPs are subsequently detached by salt.

(iii) Many animal MAPs are thermostable (**Fig. 17C**), i.e. they can be enriched by boiling the sample in presence of salt (85), whereas most other proteins will be precipitated.

(iv) The neurotubule-cosedimentation and the tubulin-coassembly approach fails in those cases, where proteins can form large complexes independently of microtubules (Freudenreich et al., manuscript in preparation). For these cases, a new approach had to be designed, whereby a neurotubule-coated nitrocellulose membrane is used as matrix for MAP-binding. This assay is based exclusively on affinity, not on sedimentability.

Using these approaches, signal-induced MAPs were purified from maize seedlings.

Two potential MAPs that respond to phytochrome. The maize coleoptile grows exclusively by cell expansion and responds to various signals such as light (9), gravity (59), and auxin (8). These growth responses are accompanied by a reorientation of cortical microtubules in the maize epidermis (56, 94). In darkness, elongation is delayed considerably, whereas it is stimulated up to fourfold upon induction of the phytochrome system. This system allows for a comparison of non-elongating cells (cultivation in darkness) versus elongating cells (cultivation under continuous far-red light to exclusively activate the phytochrome system).

A thermostable, 100-kDa protein could be detected in extracts from non-elongating, dark-grown coleoptiles. This protein coassembled with endogenous tubulin into microtubules and bound to taxol-stabilized neurotubules (65). It was immunologically related to the heat-stable 100-kDa (P_{100}) previously isolated from maize suspension cultures (85), and to the neural MAP τ.

In elongating, far-red irradiated coleoptiles, this protein, although detectable, was far less abundant. A 50-kDa protein (P_{50}) was found instead that coassembled with endogenous tubulin into microtubules and bound to

taxol-stabilized neurotubules (65). It was immunologically related to P_{100} and τ as well. However, it was not heat-stable, in contrast to the 100-kDa MAP.

Using the anti-P_{100} antisera (85), the tissue- and temporal regulation of both potential MAPs was investigated: The P_{100}-protein was detected in soluble extracts from roots and its expression and thermostability were not altered upon irradiation with far-red light. In etiolated mesocotyls, it was less abundant, but became more dominant after irradiation with far-red light. In the coleoptile, it was most abundant in the dark and it disappeared in response to far-red light, concomitantly with the ensuing elongation of the coleoptile. It reappeared, when the rate of cell elongation dropped again towards the end of coleoptile growth.

The P_{50} protein could not be detected in roots, but it was recovered, in relatively high amounts, from thermostable extracts of far-red treated mesocotyls. In coleoptiles that were irradiated with far-red light, it became detectable at the same time, when the P_{100} protein began to disappear (concomitantly with the onset of cell elongation). However, the P_{50} persisted also through later phases, when coleoptile elongation slowed down again.

Using the anti-P_{100} antibody (85), the localization of both proteins was analyzed with respect to microtubules. The situation in young coleoptiles, prior to elongation (where P_{100} was expressed, but P_{50} was not) was compared to elongating coleoptiles or coleoptiles that had already accomplished elongation, where both proteins were present. This double-immunofluorescence analysis (65) demonstrated that the P_{100} protein was predominantly associated with the nucleus, whereas the P_{50} protein was associated with cortical microtubules. This localization pattern was consistent with the results of subcellular fractionation, where P_{100} was observed to be enriched in the nuclear fraction, whereas P_{50} co-fractionated, along with a part of tubulin, with the plasma membrane (65).

Both proteins have been purified in the meantime by anion-exchange chromatography from thermostable extracts of etiolated (P_{100}) and far-red irradiated (P_{50}) tissue. Partial peptide sequences were obtained and were used to identify the proteins. P_{100} turned out to be a member of the HSP90 family of chaperone proteins, whereas the peptide sequence obtained for P_{50}, so far did not lead to the identification of this protein. Both proteins are presently cloned using a PCR-based approach. Thus, although both proteins are immunologically related, they do not originate from the same gene.

P_{50} appears to be a novel protein that becomes expressed and associated with cortical microtubules upon phyto-

chrome-induced cell elongation.

A 150-kDa MAP from tobacco. A second approach to isolate plant MAPs was stimulated by the repeated failure of several groups to find sequence homologues of animal MAPs in plants. On the other hand, the microtubule-binding- and affinity assay (**Fig. 17A,D**) demonstrates that plant MAPs can bind to animal microtubules. Moreover, fluorescent neurotubulin that is microinjected into living plant cells, is integrated swiftly into microtubules and seems to be functional in the host cell (83, 93, 95). This might indicate that microtubule-binding domains have been structurally conserved between plant and animal MAPs.

To pick up such structure-conservation, antibodies were reaised against a peptide stretch that had been conserved within the microtubule-binding domains of various neural MAPs.

This antibody did recognize several proteins in extracts of tobacco cell cultures. However, only some of these proteins exhibited true microtubule-binding as tested by microtubule co-sedimentation and affinity assays (**Fig. 17A,D**). Among those proteins, two heat-stable proteins of 130-kDa and 150-kDa apparent molecular weight were found to bind specifically and tightly to neurotubules. Both proteins were subsequently purified by thermostable extraction, anion-exchange chromatography, and gel filtration. In the course of almost two years the 150-kDa protein could be purified to amounts that were sufficient for peptide sequencing. Again, the peptide sequences suggest a novel type of protein and the corresponding gene is presently cloned by a PCR-based approach.

5. Prospects

The cytoskeletal mutants exhibit altered patterns of cytoskeletal proteins. The MAP P_{50} from maize coleoptiles is expressed during phytochrome-induced cell elongation (65). It is not clear, however, whether the trigger is phytochrome itself or whether P_{50} is responding to the enhanced cell elongation induced by the activation of phytochrome. Therefore, the pattern of expression was analyzed in rice, where coleoptile elongation is optimal in complete darkness and becomes inhibited upon activation of the phytochrome system (70). Interestingly, it is P_{50} and not P_{100} that is expressed in etiolated (elongating) rice coleoptiles, whereas in light-treated coleoptiles (where elongation is blocked), in addition to P_{50}, P_{100} (HSP90) is expressed (**Fig. 18**). In coleoptiles of the mutant *ER31*, where elongation is impaired even in darkness, the expression of P_{50} is accompanied by the expression of P_{100} (HSP90) as well (**Fig. 18**). These data indicate that expression of P_{50} is characteristic for cells that elongate - irrespective of the signal that triggers this elongation.

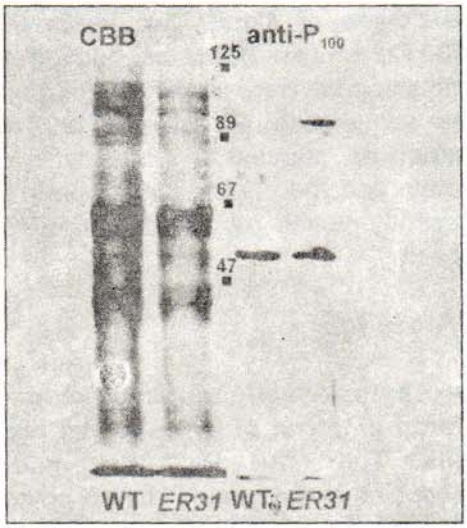

Figure 18: Expression of P_{100} (HSP90) and P_{50} in etiolated coleoptiles of wild-type and the mutant *ER31*.

In the *Yin-Yang* mutant as well, changes in the pattern of cytoskeletal proteins have been detected. A 60-kDa protein that is recognized by a monoclonal antibody directed to actin can be detected in soluble extracts of the mutant, but not in extracts of the wild type. This 60-kDa protein is also induced in maize coleoptiles as well in response to far-red light (Waller, unpublished results) cofractionates with F-actin, and seems to bind to microtubules as found in neurotubule cosedimentation assays (**Fig. 17A**) and by EPC-affinity chromatography (47). Whether the appearance of this actin-related potential MAP is the cause for the impaired cell elongation in *the Yin-Yang* epidermis, warrants further investigation.

Towards an in-vivo assay for MAP-function. To test the possible function of a protein, reconstitution systems have to be designed. Principally, cloned genes could be used for the production of transgenic plants overexpressing the respective genes (gain-of-function assay) or the respective anti-sense constructs (loss-of-function assay). Alternatively, mutants that lack certain cytoskeletal responses, could be transformed with MAP-genes in a gain-of-function assay. This approach, although unevitable for a developmental analysis, is cumbersome and, as observed for the cytoskeletal mutants, many pleiotropic effects are expected, since the cytoskeleton participates in a multitude of developmental processes.

A second approach is transient in nature and based on the responses of individual cells within the tissue context: Upon microinjection of fluorescent-labelled neurotubulin into living plant cells, the dynamics of the microtubular cytoskeleton can be immediately observed (83, 93, 95). It is now planned to coinject plant MAPs that either have been purified directly or that originate from genes that have been overexpressed in bacteria. Alternatively, the respective antibodies can be coinjected to deplete endogenous MAPs. By fusions of MAP-genes to green or red fluorescent protein, the dynamics of MAP-microtubule interaction should become visible in the living cell. These tools could then be

applied to wild-type cells or, in a gain-of-function assay, to appropriate mutants.

This approach, combining molecular biology with cellular physiology should help to understand a fundamental aspect of plant development: the coupling of signal transduction to cellular morphogenesis.

References

1. Ahmad, F.J. & Baas, P.W. (1995). J. Cell Sci. 106, 2761-2769.
2. Arumuganathan, K. & Earle, E.D. (1991). Plant Mol. Biol. Reports 9, 208-218.
3. Baskin, T.I. & Bivens, N.J. (1995). Planta 197, 514-521.
4. Bassell, G.J., Powers, C.M., Taneja, K.L. & Singer, R.H. (1994). J. Cell Biol. 126, 863-876.
5. Bergfeld, R., Speth, V. and Schopfer, P. (1988). Bot. Acta 101, 57-67.
6. Blancaflor, E.B. & Hasenstein, K.H. (1993). Planta 191, 230-237.
7. Brauner, L. & Hager, A. (1957). Naturwissenschaften 44, 429-430.
8. Briggs, W.R. (1963a). Plant Physiol. 38, 237-247.
9. Briggs, W.R. (1963b). Am. J. Bot. 50, 196-207.
10. Cande, W.J. (1990). Curr. Op. Cell Biol. 2, 301-305.
11. Chang-Jie, J. & Sonobe, S. (1993). J. Cell Sci. 105, 891-901.
12. Cholodny, N. (1927). Biol. Zentralblatt 47, 604-626.
13. Cleary, A.L. & Hardham, A.R. (1993). Plant Cell Physiol. 34, 1003-1008.
14. Cleveland, D.W. (1987). J. Cell Biol. 104, 361-383.
15. Czapek, F. (1895). Jb. Wiss. Botanik 27, 243.
16. Darwin, C. & Darwin, F. (1881). The Power of Movements in Plants. John Murray, London.
17. Ducket, C.M. & Lloyd, C.W. (1994). Plant J. 5, 363-372.
18. Durso, N.A. & Cyr, R. J. (1994). Plant Cell 6, 893-905.
19. Falconer, M.R. & Seagull, R.W. (1985). Protoplasma 128, 157-166.
20. Falconer, M.R., Donaldson, G. & Seagull, R.W. (1988). Protoplasma 144, 46-55.
21. Fukui, H. & Kobayashi, H. (1989). Development, Growth & Different. 31, 9-15.
22. Furuya, M., Pjon, Ch.J., Fujii, T. & Ito, M. (1969). Development, Growth & Different. 11, 62-76.
23. Giddings, T.H. & Staehelin, A. (1991). In: Lloyd, C.W. (editor) The Cytoskeletal Basis of Plant Growth and Form, pp. 85-99, Academic Press, London.
24. Grabski, S. & Schindler, M. (1996). Plant Physiol. 110, 965-970.
25. Green, P.B. (1980). Annu. Rev. Plant Physiol. 31, 51-82.
26. Hartmann, E. (1984). Brid. J. Hattori Bot. Lab. 55, 87-98.
27. Hasezawa, S. & Nagata, T. (1993). Protoplasma 176, 64-74.
28. Hugdahl, J.D., Bokros, C.L. & Morejohn, L.C. (1995). Plant Cell 7,

2129-2138
29. Hussey, P.J., Traas, J.A., Gull, K. & Lloyd, C.W. (1987). J. Cell Sci. 88, 225-230.
30. Iino, M. & Baskin, T.I. (1984). Plant, Cell & Environment 7, 97-104.
31. Jablonski, P.P., Elliot, J. & Williamson, R.E. (1993). Plant Science 94, 35-45.
32. Jongewaard, I., Colon, A. & Fosket, D.E. (1994). Protoplasma 183, 77-85.
33. Kreis, T. & Vale, R. (1993). Guidebook to the Cytoskeleton and Motor Proteins, pp. 101-105. Oxford University Press, Oxford.
34. Kurata, N., Nagamura, Y., Yamamoto, K., Harushima, Y., Sue, N., Wu, J., Antonio, B.A., Shomura, A., Shimizu, T., Lin, S.Y., Inoue, T., Fukuda, A., Shimano, T., Kubohi, Y., Toyama, T. Miyamoto, Y., Kirihara, T., Hayasaka, K., Miyao, A., Monua, L., Zhong, H.S., Tamura, Y., Wang, Z.-X., Momma, T., Umehara, Y., Yano, M., Sasaki, T. & Minobe, Y. (1994). Nature Genetics 8, 365-372.
35. Kutschera, U., Bergfeld, R. & Schopfer, P. (1987) Planta 170, 168-180.
36. Lambert, A.M. (1993). Curr. Op. Cell Biol. 15, 116-122.
37. Lang, J.M., Eisinger, W.R. & Green, P.B. (1982). Protoplasma 110, 5-14.
38. Laskowski, M.J. (1990) Planta 181, 44-52.
39. Ledbetter, M.C. & Porter, K.R. (1963). J. Cell Biol. 12, 239-250.
40. Lee, V.D. & Huang, B. (1990). Plant Cell 2, 1051-1057.
41. Liu, B., Marc, J., Joshi, H.C. & Palevitz, B.A. (1993). J. Cell Sci. 104, 1217-1228.
42. Lloyd, C.W. & Seagull, R.W. (1985). Trends in Biochem. Sci. 10, 476-478.
43. Lloyd, C.W. (1991). In: Lloyd, C.W. (editor) The Cytoskeletal Basis of Plant Growth and Form, pp. 245-257, Academic Press, London.
44. Maekawa, T., Ogihara, S., Murofushi, H. & Nagai, R. (1990). Protoplasma 158, 10-18.
45. Marc, J. & Palevitz, B.A. (1990). Planta 182, 626-634.
46. Mineyuki, Y., Marc, J. & Palevitz, B.A. 1988. Protoplasma 147, 200-203.
47. Mizuno, K., Koyama, M. & Shibaoka, H. (1981). J. Biochem. 89, 329-332.
48. Mizuno, K. & Suzaki, T. (1990). Bot. Mag. Tokyo 103, 435-448.
49. Mizuno, K. (1995). Protoplasma 186, 99-112.
50. Morejohn, L.C. (1994). Plant Cell 6, 1696-1699.
51. Murata, T. & Wada, M. (1991) Plant Cell Physiol. 32, 1145-1151
52. Nick, P. & Schäfer, E. (1988a). Planta 173, 213-220.
53. Nick, P. & Schäfer, E. (1988b). Planta 175, 380-388.
54. Nick, P. & Schäfer, E. (1989). Planta 179, 123-131.
55. Nick, P. (1990). Versuch über Tropismus, Querpolarität und Mikrotubuli. Faculty of Biology, Freiburg.
56. Nick, P., Bergfeld, R., Schäfer, E.

& Schopfer, P. (1990). Planta 181, 162-168.
57. Nick, P., Sailer, H. & Schäfer, E. (1990). Planta 181, 385-392.
58. Nick, P. & Schäfer, E. (1991) Planta 185, 415-424.
59. Nick, P., Schäfer, E., Hertel, R. & Furuya, M. (1991). Plant Cell Physiol. 32, 873-880.
60. Nick, P., Furuya, M. and Schäfer, E. (1991). Plant Cell Physiol. 32, 999-1006.
61. Nick, P., Schäfer, E. & Furuya, M. (1992). Plant Physiol. 91, 1302-1308.
62. Nick, P. & Furuya, M. (1993). Plant Growth Reg. 12, 195-206.
63. Nick, P. & Schäfer, E. (1994). Planta 195, 63-69.
64. Nick, P. Yatou, O., Furuya, M. & Lambert, A.M. (1994). Plant J. 6, 651-663.
65. Nick, P., Lambert, A.M. & Vantard, M. (1995). Plant J. 8, 835-844.
66. Nick, P. & Furuya, M. (1996). Plant Cell & Environm. 19, 1179-1187.
67. Nick, P. & Godbolé, R. (1997). Biol. Bulletin, in press.
68. Parness, J. & Horwitz, S.B. (1981). J. Cell Biol. 91, 479-487.
69. Pjon, Ch.J. & Furuya, M. (1967). Plant Cell Physiol. 8, 704-718.
70. Preston, R.D. (1988). Planta 174, 64-74.
71. Seagull, R.W. (1990). Protoplasma 159, 44-59.
72. Shelanski, M.L., Gaskin, F. & Cantor, C.R. (1973). Proc. Natl. Acad. Sci. USA 70, 765-768.
73. Shibaoka, H. & Hogetsu, T. (1977). Bot. Mag. Tokyo 103, 435-448.
74. Shibaoka, H. (1991). In: Lloyd, C.W. (editor) The Cytoskeletal Basis of Plant Growth and Form, pp. 159-168, Academic Press, London.
75. Shiina, N., Gotoh, Y., Nishida, E. (1992). EMBO J. 11, 4723-4731.
76. Silflow, C.D., Oppenheimer, D.G., Kopczak, S.D., Ploense, S.G., Ludwig, S.R., Haas, H. & Snustad, D.P. (1987). Dev. Genetics 8, 435-460.
77. Solomon, F., Magendantz, M. & Salzman, A. (1979). Cell 18, 431-438.
78. Sonobe, S. & Shibaoka, H. (1989). Protoplasma 148, 80-86.
79. Stoppin, V., Vantard, M., Schmit, A. & Lambert, A.M. (1994). Plant Cell 6, 1099-1106.
80. Thimann, K.V. & Biradivolu, R. (1994). Protoplasma 183, 5-9.
81. Toyomasu, T., Yamane, H., Murofushi, N. & Nick, P. (1994) Planta 194, 256-263.
82. Traas, J., Bellini, C., Nacry, P., Kronenberger, J., Bouchez, D. & Caboche, M. (1995) Nature 375, 676-677.
83. Vantard, M., Levilliers, N., Hill, A.M., Adoutte, A. & Lambert, A.M. (1990). Proc. Natl. Acad. Sci. USA 87, 8825-8829.
84. Vantard, M., Schellenbaum, P., Fellous, A. & Lambert, A.M. (1991). Biochemistry 30, 9334-9340.
85. Vantard, M., Peter, C., Fellous, A. & Schellenbaum, P. (1994). Eur. J. Biochem. 220, 847-853.
86. Wang, Q.Y. & Nick, P. (1997). Plant Physiol., submitted.
87. Went, F.W. (1928). Recueil des Travaux Botanique Néerlandais 25, 1-

116.
88. Went, F.W. & Thimann, K. (1937). Phytohormones. MacMillan, New York.
89. Williamson, R. E. (1991). Int. Rev. Cytol. 129, 135-206.
90. Wymer, C. & Lloyd, C.W. (1996). Trends in Plant Sci. 1, 222-227.
91. Yang, F., Demma, M., Warren, V., Dharmawardhane, S. & Condelis, J. (1990). Nature 347, 494-496.
92. Yasuhara, H., Sonobe, S. & Shibaoka, H. (1992). Plant Cell Physiol. 33, 601-608.
93. Yuan, M., Shaw, P.J., Warn, R.M. & Lloyd, C.W. (1994). Proc. Natl. Acad. Sci. USA 91, 6050-6053.
94. Zandomeni, K. & Schopfer, P. (1993) Protoplasma 173, 103-112.
95. Zhang, D., Waldsworth, P. & Hepler, P.K. (1990). Proc. Natl. Acad. Sci. USA 87, 8820-8824.